Theoretical study of the impact of alloy disorder on carrier transport and recombination processes in deep UV (Al,Ga)N light emitters

Robert Finn, Michael O'Donovan, Patricio Farrell, Julien Moatti, Timo Streckenbach, Thomas Koprucki, Stefan Schulz

Theoretical study of the impact of alloy disorder on carrier transport and recombination processes in deep UV (Al,Ga)N light emitters

R. Finn,[1] M. O'Donovan,[2] P. Farrell,[2] J. Moatti,[3] T. Streckenbach,[2] T. Koprucki,[2] and S. Schulz[1,4]
[1)] *Tyndall National Institute, University College Cork, Cork, T12 R5CP, Ireland*
[2)] *Weierstrass Institute (WIAS), Mohrenstr. 39, 10117 Berlin, Germany*
[3)] *Inria, Univ. Lille, CNRS, UMR 8524 - Laboratoire Paul Painlevé, F-59000 Lille, France*
[4)] *School of Physics, University College Cork, Cork, T12 YN60, Ireland*

(*Electronic mail: robert.finn@tyndall.ie)

(Dated: 20 July 2023)

Aluminium gallium nitride ((Al,Ga)N) has gained significant attention in recent years due to its potential for highly efficient light emitters operating in the deep ultra-violet (UV) range (< 280 nm). However, given that current devices exhibit extremely low efficiencies, understanding the fundamental properties of (Al,Ga)N-based systems is of key importance. Here, using a multi-scale simulation framework, we study the impact of alloy disorder on carrier transport, radiative and non-radiative recombination processes in a *c*-plane $Al_{0.7}Ga_{0.3}N/Al_{0.8}Ga_{0.2}N$ quantum well embedded in a *p*-*n* junction. Our calculations reveal that alloy fluctuations can open "percolative" pathways that promote transport for the electrons and holes into the quantum well region. Such an effect is neglected in conventional, and widely used transport simulations. Moreover, we find that the resulting increased carrier density and alloy induced carrier localization effects significantly increase non-radiative Auger-Meitner recombination in comparison to the radiative process. Thus, to avoid such non-radiative process and potentially related material degradation, a careful design (wider well, multi quantum wells) of the active region is required to improve the efficiency of deep UV light emitters.

Light emitters operating in the ultraviolet (UV) spectral range have received significant attention in recent years due to their importance for a wide range of applications.[1] A region of particular interest is the deep-UV-C wavelength window (< 280 nm), which enables for instance water purification and sterilization. Aluminium gallium nitride ((Al,Ga)N) based light emitting diodes (LEDs) are ideal candidates for such applications since their emission wavelengths can in principle be tuned across the entire UV spectrum and they do not require the use of toxic mercury. Unfortunately, the external quantum efficiency (EQE) of (Al,Ga)N-based LEDs is very low ($\leq$1%) in the deep UV-C range and multiple factors contribute to this, e.g. low light extraction efficiencies and poor carrier injection, high defect densities and thus reduced radiative recombination in the active region.[1,2]

Understanding the fundamental material and device properties is of central importance in improving the efficiency of such devices. Theory and simulation plays an important role for guiding the device design. However, III-N systems and alloys, such as (In,Ga)N, (Al,In)N but also (Al,Ga)N, exhibit in general very different properties when compared to other III-V materials, e.g. (In,Ga)As. For instance, experimental and theoretical studies reveal strong alloy fluctuation induced carrier localization effects in III-N alloys and heterostructures.[3–8] Accounting for such effects present a significant challenge for an accurate theoretical and numerical description, since a three-dimensional (3D) treatment of, for instance, a quantum well (QW), is required ideally on an atomistic level. Numerical challenges are further amplified when it comes to simulating LED structures, which require not only large 3D supercells but also self-consistent calculations. Significant progress has been made to address these questions.[6,9,10] But, in comparison to (In,Ga)N-based systems, understanding the fundamental impact of alloy fluctuations on electronic, optical and carrier transport properties in (Al,Ga)N-based QW systems is sparse.

Here, we target these questions for an $Al_{0.7}Ga_{0.3}N/Al_{0.8}Ga_{0.2}N$ QW embedded in *p*- and *n*-doped regions, thus a system relevant for deep UV (Al,Ga)N-based LEDs. The calculations build on our recently established quantum corrected multi-scale simulation framework that connects atomistic electronic structure theory with a drift-diffusion scheme to analyze carrier transport. To target recombination processes, the model is coupled with the widely used *ABC* model[11], where empirical *A*, *B* and *C* coefficients from the literature are employed. Our results indicate that alloy fluctuations can promote carrier transport through the intrinsic barriers by opening up percolative paths that are lower in energy. These pathways appear to improve the carrier injection into the QW active region – a feature that is neglected in 'conventional' calculations utilizing a virtual crystal approximation (VCA). Moreover, while we find that alloy disorder and carrier localization effects enhance radiative recombination, we find also that non-radiative Auger-Meitner recombination processes are strongly increased. The resulting increase in high energy carriers via non-radiative Auger-Meitner recombination may also lead to a degradation of the material as indicated in experimental studies.[12] As a consequence, our results suggest that alloy disorder can have a detrimental effect on the device efficiency. To reduce Auger-Meitner related processes, increasing the well width or employing multi QW (MQW) active regions to reduce the carrier density may be a way to improve quantum efficiencies in UV emitters, as the above discussed percolation paths may be exploited to distribute the carriers more evenly between MQWs.

In order to investigate the impact alloy disorder has on carrier transport and recombination processes in (Al,Ga)N-based LEDs, we describe the electronic structure of the active region by means of a empirical nearest neighbour sp^3 tight-binding

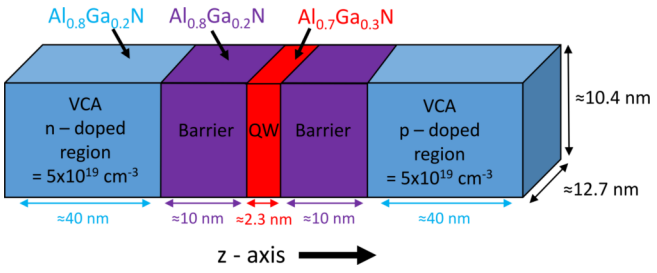

FIG. 1. Schematic illustration of the (Al,Ga)N-based *p-i-n* system underlying the simulations. The intrinsic barriers plus quantum well region is denoted as the "atomistic" mesh in the main text, while the *n*- and *p*-regions are described by a sparser device mesh.

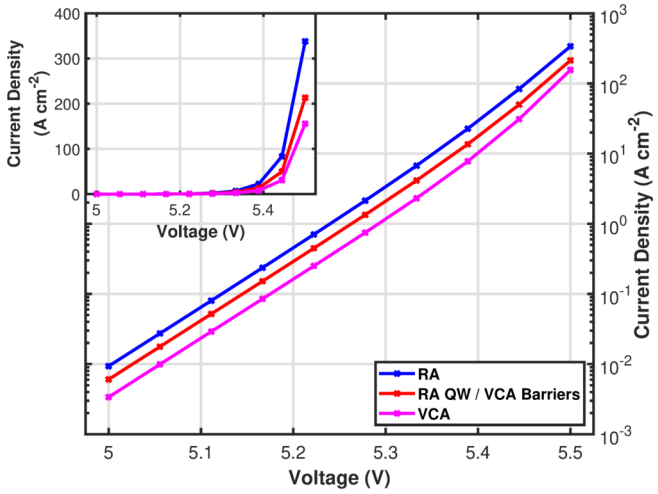

FIG. 2. (a) Current-voltage curves, on a log-scale, for an $Al_{0.7}Ga_{0.3}N/Al_{0.8}Ga_{0.2}N$ quantum well embedded in a *p-n* junction. The data are shown for simulations that (i) account for random alloy (RA) fluctuations in the well and barriers (blue), (ii) account for RA fluctuations in the well but treat the barrier in a virtual crystal approximation (VCA) (red), and (iii) use a VCA in the entire *p-i-n* structure (pink). The inset shows the I-V curves on a linear scale.

(TB) model. We note that while we treat the TB matrix elements as free parameters to reproduce hybrid-functional DFT band structures, the TB matrix could also be constructed from maximally localized Wannier functions generated from DFT[13]. This would thus provide an avenue to extend our method towards a DFT-based TB Hamiltonian. In general, our employed TB framework treats strain and polarization field fluctuations due to random alloy fluctuations with an atomistic resolution. We have recently employed the TB model to study the influence of alloy fluctuations on the electronic and optical properties of (Al,Ga)N/AlN QWs. Our work revealed that random alloy fluctuations are sufficient to lead to carrier localization effects in such systems. A detailed description of the model and electronic structure results is given in Ref. 8.

To connect our TB model to drift-diffusion (DD) simulations we have recently developed the following procedure.[10] As a first step a "local" TB Hamiltonian is constructed. By diagonalising this local Hamiltonian an energy landscape that accounts for alloy induced fluctuations in the conduction and valence band profile is obtained. This energy landscape with an atomistic resolution is mapped onto a finite element mesh using the software library `pdelib`.[14] The underlying finite element mesh has as many nodes as the atoms in the system. To target LED device simulations, the "atomistic" mesh is connected to a sparser device mesh representing *p*- and *n*-doped regions. Using localization landscape theory (LLT)[9] in conjunction with the software package `ddfermi`,[15] quantum corrected DD simulations are performed. More details about the carrier transport calculations, the mesh generation and numerical aspects can be found in Refs. 10 and 16.

The above outlined quantum corrected multi-scale simulation framework is here applied to a *p-i-n* system where the intrinsic (*i*) region contains a 2.3 nm wide $Al_{0.7}Ga_{0.3}N$ QW embedded into approximately 10 nm wide intrinsic $Al_{0.8}Ga_{0.2}N$ barriers, following the UV-C device design in Ref. 17. The atomistic mesh region describing the active region of the device has the dimensions of roughly $17.4 \times 15.1 \times 22.2$ nm^3, corresponding to $\approx$ 560,000 atoms, and is coupled with a sparser device mesh by adding 40 nm of *n*- and *p*-doped regions, respectively. The doping density is 5×10^{19} cm^{-3} following the set-up described in Ref. 18. A schematic illustration of the structure is given in Fig. 1. To connect the conduction band and valence band edges between the atomistic and the sparser mesh, we use a blend of Gaussian softening and LLT to avoid discontinuities at such an interface. Details on the Gaussian softening and the effect of LLT on the energy landscape can be found elsewhere.[10] To test the impact of the in-plane dimensions of the simulation cell and thus also the influence of the alloy microstructure on the results, the calculations have been repeated for different cell sizes (not shown). These different calculations revealed in general the same trends as reported below, so that the above detailed simulation set up gives a representative picture of the impact of alloy disorder on the carrier transport in the discussed device.

To investigate the impact alloy fluctuations have on the carrier transport and the recombination process we proceed as follows: Our starting point is a fully atomistic description, meaning that alloy fluctuations in both the intrinsic (Al,Ga)N QW and (Al,Ga)N barriers are accounted for (cf. Fig. 1). To study the impact of alloy disorder on the carrier injection, we investigate a second set-up in which alloy fluctuations in the (Al,Ga)N QW are treated on an atomistic level, however the intrinsic (Al,Ga)N barriers are described in a VCA. Finally, we employ a VCA description of the entire QW plus barrier system. This last setting is basically equivalent to one-dimensional carrier transport simulations widely employed in commercially available software packages. In order to establish a comparable VCA description of the targeted system, without introducing additional free parameters (e.g. alloy dependence and or bowing parameters of material parameters), the atomistic energy landscape is averaged over the corresponding areas (e.g. well or barrier). To achieve this averaging procedure, the QW was treated initially with Dirichlet boundary conditions so that, except from alloy fluctuation induced variations, the conduction and valence band edges are flat. A VCA description of the barriers is then

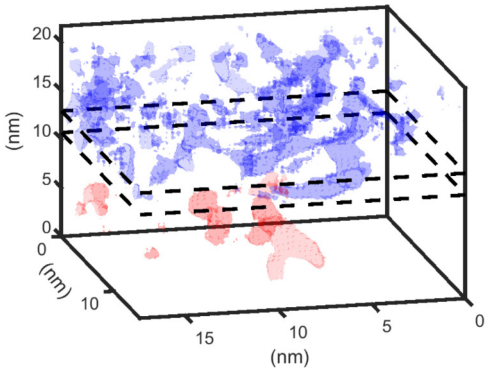

FIG. 3. 3D isosurface plot of the current density in the intrinsic (Al,Ga)N quantum well and barrier regions at a bias of 5.5 V, using the fully atomistic description. The current density for the holes (blue) and electrons (red) are plotted at 700 A cm^{-2}, reflecting locally high current densities due to alloy fluctuations; dashed black lines indicate well boundaries.

straightforward and achieved by averaging the atomistic energy landscape over the entire barrier volume. However, the QW VCA description is slightly more complicated as piezoelectric and spontaneous polarization induced built-in fields across the QW cause the band edges to slope. Thus, a volume average over the QW region is not possible. In this case, the atomistic energy landscape is averaged across each *c*-plane along the growth direction (*c*-axis). While this can lead to slight fluctuations in the energy landscape, the approach chosen here is better suited to compare the different calculations, since it avoids constructing a VCA that requires specific information on how to average e.g. material and TB parameters with composition, or to perform a separate VCA built-in field calculation.

Building on these different simulation set-ups, Fig. 2 displays the calculated current-voltage (I-V) curves of the above described (Al,Ga)N *p-i-n* structure using (i) the fully atomistic approach (RA), (ii) accounting for alloy fluctuations in the well but not the barrier (RA QW/VCA Barriers) and (iii) a VCA of the entire system. One can infer from this figure that the fully atomistic treatment gives independent of the applied voltage the highest current density, while the full VCA description of the system (well and barriers) results in the lowest density. Figure 2 also reveals that the current density, especially at lower bias values, is increased when accounting for alloy fluctuations in the barrier; this can be seen from the comparison of the I-V curves for the fully atomistic and 'partial' VCA (RA QW, VCA Barriers) treatment. Thus, our results indicate that alloy fluctuations are beneficial for the carrier injection into the QW region.

To visualise this aspect further, Fig. 3 depicts an isosurface plot of the current density in the intrinsic (Al,Ga)N QW and barrier regions, cf. Fig. 1, at a fixed bias point of 5.5 V obtained from the fully atomistic description of the system. One can infer that alloy fluctuation induced band edge energy fluctuations lead to regions of higher and lower current densities. Thus, the fluctuations in the band edge energies enable percolation paths into the active region; such pathways are absent

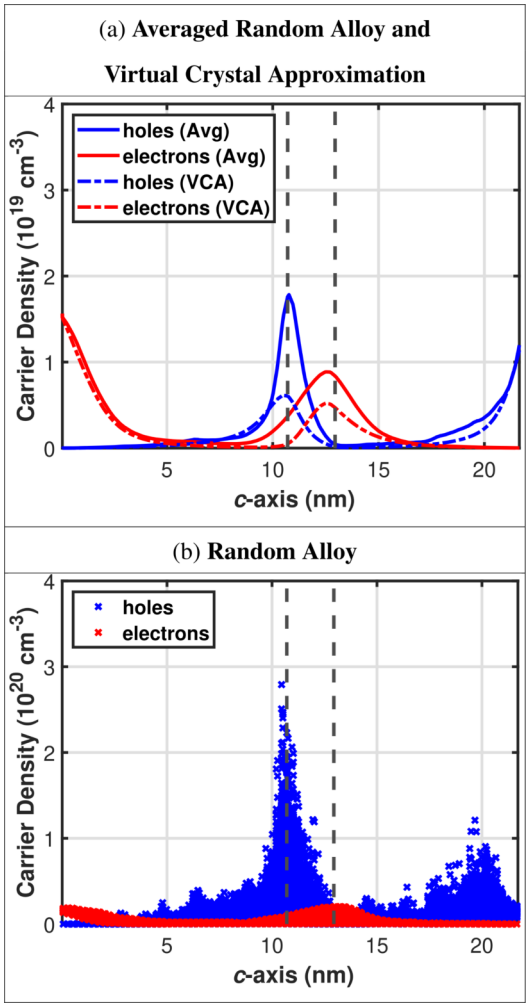

FIG. 4. Electron (red) and hole (blue) density along the *c*-axis of a $Al_{0.7}Ga_{0.3}N/Al_{0.8}Ga_{0.2}N$ quantum well embedded in a *p-i-n* junction at a bias of 5.5 V; data are shown for the intrinsic regions of the device. (a) Averaged carrier distribution of the fully atomistic calculation over each *c*-plane along the *c*-axis (solid lines), and the carrier distribution for the virtual crystal approximation (dashed lines); (b) Scatter plot of the carrier distribution in the fully atomistic calculation. The vertical dashed black lines indicate well boundaries. Note (b) is an order of magnitude larger than (a) on the *y*-axis.

in a VCA description of the system. We note that this percolation path effect has also be observed in (In,Ga)N QWs and (Al,Ga)N barriers[19–22]. We note that both electron and hole transport are affected by these percolation paths. However, due to the lower effective electron mass, the electron charge density is more smeared out, and compared to the holes, fewer regions reach the isosurface value at which the current density is plotted in Fig. 3. As a consequence of these percolation paths one expects higher carrier densities in the active region in comparison to a simulation that neglects alloy disorder. Also, as we will see below, the percolation paths can lead to an increased hole density in the intrinsic barrier on the *n*-side of the studied system. Such a situation may be beneficial for inter-well transport in (Al,Ga)N multi-QW systems as

recently reported in (In,Ga)N-based LEDs.[23]

To study the impact of alloy fluctuations on the carrier transport and recombination in (Al,Ga)N-based LED structures in further detail, Fig. 4 depicts electron and hole carrier densities above the turn-on voltage of the device, at a bias of 5.5 V. Figure 4 (a) displays the *averaged* carrier density, over each *c*-plane, for the random alloy system along the *c*-axis (growth direction) together with the VCA data which neglects alloy disorder. When comparing the averaged random alloy data with the VCA results, it becomes clear that *(on average)* both electron and hole carrier densities are increased in the well when taking alloy fluctuations into account. Figure 4 (a) indicates that the *average* hole charge density does not leak as much into the intrinsic (Al,Ga)N barrier material on the *n*-side of system (region below 10.7 nm), when compared to the hole density profile in VCA; one may attribute this to alloy induced hole localization effects which are not accounted for by the VCA description. The *average* electron density extends further into the (Al,Ga)N barrier region on the *p*-side (region above 13 nm) when compared to the VCA data; we relate this to the effect that alloy disorder and quantum corrections effectively reduce the quantum confinement between well and barrier and that the electrons are less strongly affected by alloy induced carrier localization effects as already seen in (In,Ga)N-based systems.[10] However, it must be noted that the random alloy data in Fig. 4 (a) are averaged over each *c*-plane. Thus, while on average the hole density may be smaller in e.g. the intrinsic barrier of the *n*-region when compared to VCA, local alloy regions may have high hole densities. To shed light onto this behavior, Fig. 4 (b) displays a scatter plot of the carrier densities along the *c*-axis in the intrinsic (Al,Ga)N regions. The symbols give the carrier density at each lattice site within the respective *c*-planes. Figure 4 (b) reveals strong fluctuations in the *local* densities which may be an order of magnitude higher than the *average* densities displayed in Fig. 4 (a). The *local* hole carrier density is also noticeably higher when compared to the electrons. In general, due to the higher effective mass, carrier localization for holes is more pronounced when compared to electrons.[8] Therefore, we conclude that percolative pathways, can promote easier transport of the carriers through the barriers. Thus, holes may transport to the *n*-side of the system more easily when compared to predictions from a VCA model. This aspect is of interest when designing multi-QW-based (Al,Ga)N LEDs, since it can help with a more equal distribution of holes between the wells, and thus be important for recombination processes.

Equipped with this information we turn our attention now to the recombination process in the system. To do so we employ the widely used *ABC* model. In the following we mainly focus our attention on the radiative and Auger-Meitner (non-radiative) processes; with increased current densities radiative and non-radiative Auger-Meitner processes become dominant over Shockley-Read-Hall (SRH) recombination as these contributions scale with carrier density n as $\propto n^2$ (radiative) and $\propto n^3$ (Auger-Meitner) compared to $\propto n$ (SRH). We note that defect related non-radiative processes, such as SRH and trap assisted tunnelling (TAT) processes can also affect the device performance of UV-C (Al,Ga)N-based LEDs significantly. While we take SRH into account, TAT processes have not been considered here but could be accounted for as a SRH-like process with different capture rates as detailed in Ref. 24. Turning to radiative and Auger-Meitner (non-radiative) recombination rates, Fig. 5 depicts these rates calculated (i) including random alloy fluctuations and thus carrier localization effects and (ii) using VCA for the entire system, consequently excluding alloy disorder. Figure 5 displays the random alloy (RA) data averaged over each *c*-plane. We stress that the recombination rates are calculated using the *local* carrier density data, thus accounting for the effect that locally one may encounter both high electron and hole densities. The required radiative (B) and Auger-Meitner (C_{nnp} and C_{npp}) recombination coefficients are taken from Ref. 18. We note that building on this often used carrier density dependent recombination model, the wave function character of electrons and holes is not taken into account. While the symmetry of the wave functions can affect radiative and non-radiative recombination rates, analyzing the spatial overlap of electron and hole charge density provides first insight into the impact of alloy disorder on the recombination rates. Comparing the atomistic calculation with the VCA data it becomes clear that both radiative and non-radiative contributions are enhanced by alloy disorder since this can improve the carrier injection but also induce carrier localization in the wells. But, upon further inspection, Fig. 5 reveals that the non-radiative rate increases more strongly when compared to the radiative. In the VCA the ratio of radiative to non-radiative peak values is $r^{\mathrm{VCA}} \approx 19$ while in the atomistic simulation it is $r^{\mathrm{RA}} \approx 2$ at a bias of 5.5 V. In general, and using the *ABC* model[11] here as a starting point, the radiative recombination contributes with Bn^2 while the Auger-Meitner non-radiative rate with Cn^3, where n is the carrier density. Thus, when alloy disorder increases the carrier density in local regions of the well, the Auger-

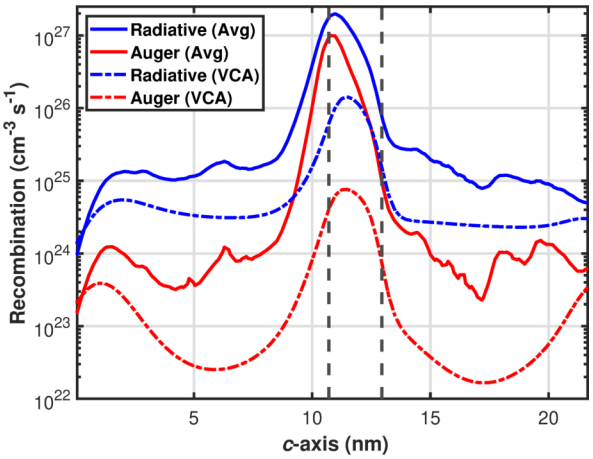

FIG. 5. Radiative and Auger-Meitner non-radiative recombination rates along the *c*-axis of the $Al_{0.7}Ga_{0.3}N/Al_{0.8}Ga_{0.2}N$ *p-i-n* system at a bias of 5.5 V; the data are shown for the intrinsic regions of the device. Solid lines: results from the atomistic calculations taking alloy fluctuations into account (averaged over each *c*-plane). Dashed lines: data obtained from a virtual crystal approximation of the same system; vertical dashed black lines indicate well boundaries.

Meitner rate is expected to increase more quickly than the radiative rate. Moreover, the Auger-Meitner rate is a three-particle process and has basically two contributions, namely an electron-electron-hole and a hole-hole-electron process.[25] Given that alloy induced carrier localization effects are significant for holes, locally the hole-hole wave function overlap is (strongly) increased. In turn this can result in increased Auger-Meitner rates.[26] Taking all this together, alloy disorder and related carrier localization effects are expected to lead to a significant increase of the non-radiative Auger-Meitner effect and thus have a detrimental effect on the performance of (deep) UV LEDs; a similar effect has been seen (In,Ga)N-base LEDs[22]. Moreover, strong Auger-Meitner non-radiative recombination may also lead to material degradation effects in deep-UV LEDs, as recently indicated in experiments.[12,24]

In summary, using a quantum corrected multi-scale simulation framework, we presented a detailed analysis of the impact of alloy fluctuations on carrier transport and recombination processes in an $Al_{0.7}Ga_{0.3}N/Al_{0.8}Ga_{0.2}N$ single quantum well system embedded in a *p-n* junction. Understanding the fundamental properties of such systems provides useful insight into the physics of deep UV light emitters. Our results show that alloy disorder can lead to improved carrier injection into the active region, i.e. quantum well, through percolative pathways. Also, these pathways can give rise to higher hole densities in the intrinsic region near the *n*-side of a device, an aspect of potential interest for tailoring inter-well transport in (Al,Ga)N-based multi quantum well systems. In general, these percolation effects are not captured by standard virtual crystal approximations employed in many commercially available carrier transport simulation packages. Moreover, we find an increase in the carrier density in the well which is accompanied by alloy induced carrier localization effects. In comparison to virtual crystal simulations, both radiative and non-radiative Auger-Meitner recombination processes are increased. We attribute this to alloy induced carrier localization effects, resulting in high local carrier densities which affect the Auger-Meitner effect more strongly than the radiative process. Moreover, the high energy of such Auger-Meitner generated carriers may lead to a degradation of the material and thus an enhancement of Shockley-Read Hall recombination. Overall, our results indicate that alloy disorder opens up percolative pathways improving carrier transport, but the enhanced Auger effect can have a detrimental effect on the efficiency of the device. While we have focused here on relatively high Al contents in the well and barrier, the above drawn conclusions are also expected to hold for systems with lower Al contents, given that our recent atomistic studies reveal that even at only 10% Al in (Al,Ga)N hole localization effects are observed. Thus, in general a careful design of the active region of an UV LED, e.g. by using wider wells as discussed in recent literature[27,28] or multi quantum wells by exploiting percolation pawthways to improve the interwell transport, is necessary to reduce non-radiative recombination processes and prevent material damage.

This work received funding from the Sustainable Energy Authority of Ireland and the Science Foundation Ireland (Nos. 17/CDA/4789, 12/RC/2276 P2 and 21/FFP-A/9014), the Leibniz competition 2020, Leibniz competition 2022 (UVSimTec, K415/2021) as well as the Labex CEMPI (ANR-11-LABX-0007-01).

The data that support the findings of this study are available from the corresponding author upon reasonable request.

[1] M. Kneissl, T.-Y. Seong, J. Han, and H. Amano, "The emergence and prospects of deep-ultraviolet light-emitting diode technologies," Nat. Photonics **13**, 233 (2019).

[2] H. Amano, R. Collazo, C. De Santi, S. Einfeldt, M. Funato, J. Glaab, S. Hagedorn, A. Hirano, H. Hirayama, R. Ishii, Y. Kashima, Y. Kawakami, R. Kirste, M. Kneissl, R. Martin, F. Mehnke, M. Meneghini, A. Ougazzaden, P. J. Parbrook, S. Rajan, P. Reddy, F. Römer, J. Ruschel, B. Sarkar, F. Scholz, L. J. Schowalter, P. Shields, Z. Sitar, L. Sulmoni, T. Wang, T. Wernicke, M. Weyers, B. Witzigmann, Y.-R. Wu, T. Wunderer, and Y. Zhang, "The 2020 UV emitter roadmap," J. Phys. D: Appl. Phys **53**, 503001 (2020).

[3] S. F. Chichibu, A. Uedono, T. Onuma, B. A. Haskell, A. Chakraborty, T. Koyama, P. T. Fini, S. Keller, S. P. DenBaars, J. S. Speck, U. K. Mishra, S. Nakamura, S. Yamaguchi, S. Kamiyama, H. Amano, I. Akasaki, J. Han, and T. Sota, "Origin of defect-insensitive emission probability in In-containing (Al,In,Ga)N alloy semiconductors," Nature Mater. **5**, 810 (2006).

[4] S. Schulz, M. A. Caro, and E. P. O'Reilly, "Impact of cation-based localized electronic states on the conduction and valence band structure of $Al_{1-x}In_xN$ alloys," Appl. Phys. Lett. **104**, 172102 (2014).

[5] S. Schulz, M. A. Caro, C. Coughlan, and E. P. O'Reilly, "Atomistic anaylsis of the impact of alloy and well width fluctuations on the electronic and optical properties of InGaN/GaN quantum wells," Phys. Rev. B **91**, 035439 (2015).

[6] A. Di Vito, A. Pecchia, A. Di Carlo, and M. Auf Der Maur, "Simulating random alloy effects in III-nitride light emitting diodes," J. Appl. Phys. **128**, 041102 (2020).

[7] C. Weisbuch, S. Nakamura, Y.-R. Wu, and J. S. Speck, "Disorder effects in nitride semiconductors: impact on fundamental and device properties," Nanophotonics **10(1)**, 3–21 (2021).

[8] R. Finn and S. Schulz, "Impact of random alloy fluctuations on the electronic and optical properties of (Al,Ga)N quantum wells: Insights from tight-binding calculations," J. Chem. Phys. **157**, 244705 (2022).

[9] M. Piccardo, C.-K. Li, Y.-R. Wu, J. S. Speck, B. Bonef, R. M. Farrell, M. Filoche, L. Martinelli, J. Peretti, and C. Weisbuch, "Localization landscape theory of disorder in semiconductors. II. Urbach tails of disordered quantum well layers," Phys. Rev. B **95**, 144205 (2017).

[10] M. O'Donovan, D. Chaudhuri, T. Streckenbach, P. Farrell, S. Schulz, and T. Koprucki, "From atomistic tight-binding theory to macroscale drift-diffusion: Multiscale modeling and numerical simulation of uni-polar charge transport in (In,Ga)N devices with random fluctuations," J. Appl. Phys. **130**, 065702 (2021).

[11] J. Piprek, "Efficiency droop in nitride-based light-emitting diodes," Phys. Status Solidi A **207**, No. 10, 2217–2225 (2010).

[12] J. Glad, J. Ruschel, N. L. Bloch, H. K. Cho, F. Mahnke, L. Sulmoni, M. Guttmann, T. Wernicke, M. Weyers, S. Einfeldt, and M. Kneissl, "Impact of operation parameters on the degradation of 233 nm AlGaN-based far UVC LEDs," J. Appl. Phys. **131**, 014501 (2022).

[13] M. Wahn and J. Neugebauer, "Generalized Wannier functions: An efficient way to construct ab-initio tight-binding parameters for group-III nitrides," phys. stat. sol. (b) **243**, No. 7, 1583–1587 (2006).

[14] J. Fuhrmann, T. Streckenbach, *et al.*, "pdelib: A finite volume and finite element toolbox for pdes. [software]." Version: 2.4.20190405 (Weierstrass Institute (WIAS), `http://pdelib.org`, 2019).

[15] D. H. Doan, P. Farrell, J. Fuhrmann, M. Kantner, T. Koprucki, and N. Rotundo, "ddfermi – a drift-diffusion simulation tool," ddfermi – a drift-diffusion simulation tool (Weierstrass Institute (WIAS), doi: `http://doi.org/10.20347/WIAS.SOFTWARE.DDFERMI`, 2020).

[16] P. Farrell, N. Rotunda, D. H. Doan, M. Kantner, J. Fuhrmann, and T. Koprucki, "Mathematical Methods: Drift-Diffusion Models," in *Handbook of Optoelectronic Device Modeling and Simulation*, Vol. 2, edited by J. Piprek (CRC Press, 2017) Chap. 50, p. 733.771.

[17] F. Römer, M. Guttmann, T. Wernicke, M. Kneissl, and B. Witzigmann, "Ef-

fect of inhomogeneous Broadening in Ultraviolet III-Nitride Light-Emitting Diodes," Materials **14**, 7890 (2021).

[18]H.-T. Shen, Y.-C. Chang, and Y.-R. Wu, "Analysis of Light-Emission Polarization Ratio in Deep-Ultraviolet Light-Emitting Diodes by Considering Random Alloy Fluctuations with the 3D k.p Method," Phys. Status Solidi **16**, 2100498 (2022).

[19]C.-K. Wu, C.-K. Li, and Y.-R. Wu, "Percolation transport study in nitride based LED by considering the random alloy fluctuation," J. Comp. Elec. **14**, 416–424 (2015).

[20]A. A. Browne, M. N. Fireman, B. Mazumder, L. Y. Kuritzky, Y.-R. Wu, and J. S. Speck, "Vertical transport through AlGaN barriers in heterostructures grown by ammonia molecular beam epitaxy and metalorganic chemical vapor deposition," Semicond. Sci. Technol. **32**, 025010 (2017).

[21]K. S. Qwah, M. Monavarian, G. Lheureux, J. Wang, Y.-R. Wu, and J. S. Speck, "Theoretical and experimental investigations of vertical hole transport through unipolar AlGaN structures: Impacts of random alloy disorder," Appl. Phys. Lett. **117**, 022107 (2020).

[22]T.-J. Yang, R. Shivaraman, J. S. Speck, and Y.-R. Wu, "The influence of random indium alloy fluctuations in indium gallium nitride quantum wells on the device behavior," J. Appl. Phys. **116**, 113104 (2014).

[23]C. Lynsky, G. Lheureux, B. Bonef, K. S. Qwah, R. C. White, S. P. DenBaars, S. Nakamura, Y.-R. Wu, C. Weisbuch, and J. S. Speck, "Improved Vertical Carrier Transport for Green III-Nitride LEDs Using (In,Ga)N Alloy Quantum Barriers," Phys. Rev. Applied **17**, 054048 (2022).

[24]N. Roccato, F. Piva, C. D. Santi, M. Buffolo, M. Fregolent, M. Pilati, N. Susilo, D. H. Vidal, A. Muhin, L. Sulmoni, T. Wernicke, M. Kneissl, G. Meneghesso, E. Zanoni, and M. Meneghini, "Modeling the electrical degradation of AlGaN-based UV-C LEDs by combined deep-level optical spectroscopy and TCAD simulations," Appl. Phys. Lett. **122**, 161105 (2023).

[25]E. Kioupakis, D. Steiauf, P. Rinke, K. T. Delaney, and C. G. V. de Walle, "First-principles calculations of indirect Auger recombination in nitride semiconductors," Phys. Rev. B **92**, 035207 (2015).

[26]J. M. McMahon, E. Kioupakis, and S. Schulz, "Atomistic analysis of Auger recombination in *c*-plane (In,Ga)N/GaN quantum wells: Temperature-dependent competition between radiative and nonradiative recombination," Phys. Rev. B **105**, 195307 (2022).

[27]G. Muziol, H. Turski, M. Siekacz, K. Szkudlarek, L. Janicki, M. Baranowski, S. Zolud, R. Kudrawiec, T. Suski, and C. Skierbiszewski, "Beyond Quantum Efficiency Limitations Originating from the Piezoelectric Polarization in Light-Emitting Devices," ACS Photonics **6**, 1963–1971 (2019).

[28]B. Witzigmann, F. Römer, M. Martens, C. Kuhn, T. Wernicke, and M. Kneissl, "Calculation of optical gain in AlGaN quantum wells for ultraviolet emission," AIP Advances **10**, 095307 (2020).